Increasing the distinctiveness of hand vein images by Oriented Gradient Maps

Liming Chen[1] Di Huang[1] Hmida Chiheb[1] Chokri Ben Amar[2]

[1]Université de Lyon, Ecole Centrale Lyon
CNRS, *LIRIS UMR 5205*
36 Avenue Guy de Collongue
69134, Ecully, France
{firstname.lastname}@ec-lyon.fr

[2]Université de Sfax
Ecole Nationale d'Ingénieur de Sfax
REGIM
3038, Sfax, Tunisie
Chokri.BenAmar@enis.rnu.tn

Abstract: Hand vein pattern as a biometric trait for people identification has attracted an increasing interest in the recent years thanks to its properties of uniqueness, permanence, non-invasiveness and strong immunity to forgery. In this paper, we propose to make use of Oriented Gradient Maps (OGMs), that we previously proposed for face recognition using the term of Perceived Facial Images (PFIs), to represent Near-Infrared (NIR) hand dorsa vein images and to highlight the distinctiveness of hand vein patterns. Using a holistic approach through both the popular PCA and LDA, we benchmarked the proposed hand vein representations on the NCUT dataset of 2040 hand vein images and demonstrated the effectiveness of the proposed hand vein representations.

1 Introduction

Reliable people identification is a key issue for greater security in today's societies. Driven mainly by an increasing need for security against terrorist activity, sophisticated crimes and electronic frauds, biometrics-based solutions, which consist of utilizing people physiological characteristics (e.g. face, iris, fingerprint, etc.) or behavioral features (e.g. voiceprint, gait, etc.), have witnessed an accelerated pace of growth in the global market of security over the last decades. As compared to traditional methods for people identification (ID card, swipe-card, PIN code, etc.), biometric solutions generally offer the advantages such as uniqueness, permanence and difficulty of falsification.

In this paper, we propose to study an emerging biometric trait, namely dorsal hand veins, for the purpose of people identification. Anatomically, veins are the blood carrying vessels interweaved with muscles and bones; the prime function of vascular system is to supply oxygen to the body parts; the spatial arrangement of the vascular network in the human body is quite stable and unique, the pattern of vein is unique to every individual, even between identical twins [KuHG09]. In this work, we are interested by the vein patterns on the dorsal part of the hand for people identification as they are distinctly visible and easy to acquire and process. As compared to other popular biometric traits, such as face or fingerprint, hand vein patterns as biometric trait offer some unmatched advantages, in particular the following ones:

- Direct liveness test. As hand veins are imaged using far or near infrared light to capture temperature differences between the flow of hot blood in the veins and the surrounding skin, they can only be imaged on live body and images taken on a non live hand cannot capture its vein spatial arrangement ;

- Safety. As the patterns of blood vessels are hardwired underneath the skin at birth. They are much harder for intruders to forge.

Vein pattern as biometric trait is relatively recent. It was not exploited until 1990 when MacGregor and Welford [MaWe91] came up with a system called "vein check" for people identification. Despite the vast vascular network in the human body, hand veins are largely favored for their simplicity of processing and there exists an increasing body of work over the past decade, using hand vein patterns of the palmer part [MaSp07], the dorsal part [LiFa04, ZhWW08, KuPr09] or finger veins [MiNM04].

Most work in the literature propose first to segment the region of interest (ROI) and the hand subcutaneous vascular network from hand vein images, and then to extract local geometric features for matching, making use of the positions and angles of short straight vectors [CrSm95], dominant points [LiFa04], endpoints and crossing points [WZYZ06], vein minutiae and knuckle shape [KuHF09]. While all these approaches demonstrate reasonable recognition accuracy on small datasets ranging from 32 [LiFa04] to 100 subjects [KuVe09, KuHG09], they suffer from the fact that local geometric features don't capture the full differences of vein networks among subjects. In this paper, we propose a holistic approach to account for the variations of hand-dorsa vein patterns. NIR images are used to capture vascular arrangement of hand veins on the back part of the hand for NIR imaging technique is shown to be relatively tolerant to the external environment and the subject's medical condition [WaLe06][ZhWW07]. Furthermore, as raw NIR hand dorsa vein images are rather rough and unclear on the spatial arrangement of hand veins, we also propose a new texture descriptor, subsequently called Oriented Gradient Maps (OGM), to highlight their network structures. Significant experiments were carried out on a dataset of 102 subjects having left and right hand dorsa vein images and the results demonstrate that the proposed OGMs significantly improve the recognition accuracies as compared to direct use of raw NIR hand vein images.

This paper is organized as follows. Section 2 describes the principle and the system setup for the acquisition of hand-dorsa vein images. Section 3 introduces our human vision inspired Oriented Gradient Maps (OGMs) as a suitable intermediate representation of hand vein images. Section 4 presents and discusses the experimental results. Section 5 concludes the paper.

2 Acquisition of hand dorsa vein images.

Hand veins can be imaged either using Far-Infrared (FIR) Imaging techniques or Near-Infrared (NIR) Imaging techniques, thereby providing a contact-less and non-invasive data acquisition approach. Wang and Leedham [WaLe06] conducted a study in depth comparing FIR and NIR imaging techniques for vein pattern biometrics and concluded that FIR imaging techniques are sensitive to ambient conditions, i.e. temperature and humidity, and human body condition and does not provide a stable image quality. On the other hand, they showed that NIR imaging produces good quality images and is more tolerant to changes in environmental and body condition. In this work, hand dorsa vein images were captured using a NIR based system developed by [ZhWW07, WLCS10].

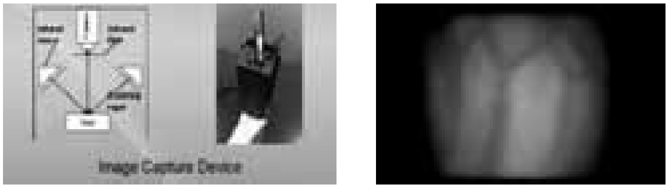

(a) (b)

Figure 1 – (a) The NIR imaging-based system setup; (b) a sample image of hand dorsa vein.

Fig.1 (a) illustrates the system setup where an array of LED lamps is used to shine infrared light onto the back of the hand. Because the incident infrared light can penetrate into the biological tissue to approximately 3 mm depth and the venous blood absorbs and scatters more the incident infrared radiation than the surrounding tissue, vein patterns can be imaged by a CCD camera with an attached IR filter where vein appears darker. To avoid major hand vein image registration issues, a handle is also defined at the bottom of the device to position the hand. The hand vein images are thus roughly aligned. Fig.1 (b) illustrates a hand dorsa vein image so captured with a resolution of 640 by 480.

Using such a setup, a dataset of 2040 hand vein images was acquired under natural lighting condition (indoor office environment) implemented by Wang et al. [ZhWW08]. In the subsequent, this dataset is called North China University of Technology hand-dorsa vein dataset or in short NCUT hand-dorsa vein dataset. Specifically, both 10 right and left hand vein images were acquired from 102 subjects, aged from 18 to 29, of which 50 were male and 52 female. This makes the dataset one of the largest ones in the field of hand vein biometrics. As the vein pattern is best defined when the skin on the back of the hand is taut, subjects were asked to clench their fist when acquiring their hand dorsa vein patterns. While there are no major lighting condition changes, slight lighting variations still can occur for hand-dorsa vein images were acquired at different time moment.

As we can see from Fig.1 (b), major hand vein patterns are captured and appear darker within the image. Widths of these vein profiles vary in the range of 30 to 50 pixels. Though the vein spatial arrangements are visible but they are not so distinguishable from the background of bio-tissue. Furthermore, local features, in terms of edge points and cross points, are very few and vary from 5 to 10, thus making local feature-based approach questionable for their discrimination power.

3 Oriented Gradient Maps (OGMs)

To increase the distinctiveness of hand-dorsa vein patterns, we propose to use *Oriented Gradient Maps* (OGM), previously named Perceived Facial Images (PFIs), proposed and applied successfully to 3D face recognition [HWAW11].

The goal of OGMs is to give a visual representation simulating the human visual perception. OGMs were inspired by the study of Edelman et al. [EdIP97], who proposed a representation method of complex neurons in primary visual cortex. The complex neurons respond to a gradient at a particular orientation and spatial frequency, but the gradient location is allowed to shift in a small receptive field rather than being precisely localized.

3.1 Representation of the complex neuron response

The proposed representation aims at simulating the response of complex neurons and it is based on a convolution of gradients in specific directions in a given circular neighborhood *R*. The precise radius value of the circular area needs to be fixed experimentally. The response of a complex neuron at a given pixel location is its gradient maps in different orientations convolved with a Gaussian kernel.

Specifically, given an input image *I*, a certain number of gradient maps G_1, G_2, …, G_o, one for each quantized direction *o*, are first computed. They are defined as:

$$G_o = \left(\frac{\partial I}{\partial o}\right)^+ \tag{1}$$

The '+' sign means that only positive values are kept to preserve the polarity of the intensity changes, while the negative ones are set to zero.

Each gradient map describes gradient norms of the input image in a direction *o* at every pixel location. We then simulate the response of complex neurons by convolving its gradient maps with a Gaussian kernel *G*. The standard deviation of *G* is proportional to the radius of the given neighborhood area, *R*, as in (2).

$$\rho_o^R = G_R * G_o \tag{2}$$

The purpose of the convolution with Gaussian kernels is to allow the gradients to shift within a neighborhood without abrupt changes.

At a given pixel location (*x*, *y*), we collect all values of the convolved gradient maps at that location and form the vector $\rho^R(x, y)$ thus having a response value of complex neurons for each orientation *o*.

$$\rho^R(x,y) = \left[\rho_1^R(x,y), \cdots, \rho_O^R(x,y)\right]^t \tag{3}$$

This vector, $\rho^R(x, y)$, is further normalized to unit norm vector, that is called in the subsequent *response vector* and denoted by ρ^R.

3.2 Oriented Gradient Maps (OGMs) by response vectors

Now a raw image can be represented by its perceived values of complex neurons according to the response vectors. Specifically, given a raw NIR hand-dorsa hand vein image *I*, we generate an Oriented Gradient Map (OGM) J_o using complex neurons for each orientation *o* defined as in (4).

$$J_o(x,y) = \underline{\rho}_o^R(x,y) \tag{4}$$

Fig.2 illustrates such a process applied to a NIR hand-dorsa vein image. In our work, we generate 8 OGMs for 8 quantized directions. Instead of original NIR hand-dorsa images, these OGMs are thus used for matching in identification based on hand vein biometrics.

3.3 The properties of distinctiveness and invariance

The proposed OGMs potentially offer high distinctiveness as they highlight the details of local shape or texture changes. Meanwhile, they also possess some interesting properties of robustness to affine lighting variations as well as affine shape transformations.

When applied to texture images, e.g. NIR hand dorsa-vein images, the proposed OGMs offer the property of being robust to affine lighting transformations. Indeed, an OGM *Jo* is simply the normalized convolved texture gradient map at the orientation o according to (4), while monotonic lighting changes often adds a constant intensity value, as a result, it does not affect the computation of gradients. Moreover, a change in image contrast in which the intensities of all pixels are multiplied by a constant will result in the multiplication of gradient computation; however, this contrast change will be also cancelled by the normalization of the response vector. Similarly, when applied to range data, OGMs are invariant to affine geometric transformations leading to tolerance to pose changes.

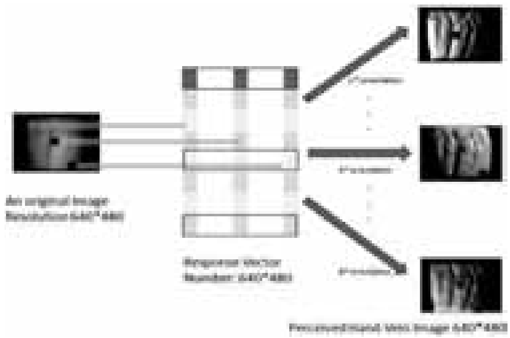

Figure 2 - OGMs describing the perceived a NIR hand-dorsa vein image in 8 orientations

The proposed OGMs can be made even rotation invariant if we quantize the directions starting from the principal gradient direction of all the gradients within a certain neighborhood. Nevertheless, we don't perform such rotation normalization for saving computational cost as NIR hand vein images in the NCUT dataset were already roughly aligned.

4 Experiments

The discrimination power of OGMs for NIR hand-dorsa vein images was experimentally evaluated using the NCUT dataset. Recall that this dataset is one of the largest datasets on NIR hand-dorsa vein images as it encompasses 10 right hand vein images and 10 left hand vein images for each of the 102 subjects, thus making up a dataset of 2040 images.

4.1 Experimental setup

As it was found that the hand vein pattern is unique to some level for each person and each hand [Bada06], we thus considered three different experimental setups, namely, i) left hand vein images are only used for the gallery and probes, ii) right hand vein images are only used for the gallery and probes, iii) left and right hand vein images are both used for the gallery an probes but as if we had 204 subjects each of which has 10 images.

As described already in section 2, all the hand-dorsa vein images were roughly aligned due to the system setup. They also have very small lighting variations as they were recorded on indoor office environment. Furthermore, each hand vein image displays very little number of local features in terms of edge points and cross points, ranging from 5 to 10. We thus propose to apply a holistic approach to analyze the discrimination power of the OGMs as compared to the original raw hand-dorsa vein images. Specifically, the popular PCA and LDA [DuHS01] were directly applied to hand vein images and their OGMs, respectively. Then their individual performances were analyzed and compared, thereby giving light on their respective discrimination power. Recall that PCA (Principal Component Analysis) seeks an optimal subspace maximizing the data variance while LDA (Linear Discriminant Analysis) finds a subspace that best discriminates among classes and requires class labels. They were widely applied to face recognition, giving birth to eigenfaces and Fischer faces, respectively, as holistic facial representation.

PCA and LDA both require learning data to seek the optimal subspace. In this work, vein image data from 51 subjects, thus half of the 102 subjects composing the dataset, were used for identifying the optimized subspace in which final matching was carried out using simple Euclidean distance. The remaining vein images from the other 51 subjects were then used for testing. Specifically, for each of the three experimental setup, both identification (one-to-many matching) and verification (one-to-one matching) scenarios were evaluated. For the identification scenario, two vein images out of ten were arbitrarily selected and placed in the gallery, the remaining 8 vein images for testing, thereby generating a rank one recognition rate as the indicator of performance. Now for verification scenario, all matching pairs from the testing data were evaluated, thus using ROC curve as the indicator of performance.

Furthermore, to check the generalization skill of the proposed method, each experimental setup was cross-validated 100 times, using each time vein data from different 51 subjects for training and the remaining vein data for testing.

4.2 The results

Tables 1 to 3 give the recognition rates of PCA compared with LDA for the aforementioned three setups, when they are applied to left hand vein images, right hand vein images and left and right hand vein images as if they were different persons, respectively. Remark that the optimization of the LDA subspace generally requires to apply first PCA so that computation of generalized eigen values are feasible. We thus also compared the performance of PCA with LDA when the variance kept from the learning dataset is increased from 80% to 95%. Meanwhile, for reason of space limitation, we only give in the following tables best results achieved when 95% variance of learning data is kept.

	PCA			LDA		
Variance	Recognition Rate	Standard Deviation	Accuracy at FAR = 0,1 %	Recognition Rate	Standard Deviation	Accuracy at FAR = 0,1 %
95 %	67.28 %	1.69	65 %	78.99 %	1.49	89 %

Table 1 - Recognition rates of PCA and LDA applied to left hand vein images.

	PCA			LDA		
Variance	Recognition Rate	Standard Deviation	Accuracy at FAR = 0,1 %	Recognition Rate	Standard Deviation	Accuracy at FAR = 0,1 %
95 %	66.65 %	1.94	65 %	79.47 %	1.36	78 %

Table 2 - Recognition rates of PCA and LDA applied to right hand vein images.

LDA demonstrates its effectiveness as compared to PCA as it improves more than 10% of the performance of PCA and reaches 79% recognition rate for both left and right hand vein images. In verification scenario, the best performance, 89% verification rate with FAR fixed at 0.1%, is also attained by LDA when keeping 95% variance of learning data.

	PCA			LDA		
Variance	Recognition Rate	Standard Deviation	Accuracy at FAR = 0,1 %	Recognition Rate	Standard Deviation	Accuracy at FAR = 0,1 %
95 %	65.96 %	1.75	65 %	77.99%	1.50	89 %

Table 3 - Recognition rates of PCA and LDA applied to left and right hand vein images as if they were different persons.

	PCA			LDA		
Orientation	Left hand	Right hand	L and R hand as diff. pers.	Left hand	Right hand	L and R hand as diff. pers.
1	61.26 %	62.00 %	61.12 %	71.98 %	77.87 %	73.40 %
2	66.24 %	68.78 %	65.36 %	72.82 %	79.55 %	74.28 %
3	71.26 %	78.55 %	72.21 %	75.63 %	81.79 %	77.45 %
4	65.21 %	67.62 %	64.12 %	74.79 %	78.43%	74.03 %
5	60.24 %	61.34 %	59.32 %	70.86 %	72.97%	71.91 %
6	62.48 %	63.02 %	60.32 %	73.38 %	77.87%	73.28 %
7	70.64 %	72.54 %	70.06 %	75.07 %	77.26%	75.73 %
8	62.18 %	64.34 %	60.87 %	72.55 %	74.79%	72.67 %
Fusion	**69.84 %**	**71.86 %**	**69.36 %**	**83.27 %**	**82.34%**	**82.96 %**

Table 4 - Recognition rates of PCA and LDA applied to left and right hand vein OGMs while keeping 95% variance of learning data.

Now we come to analyze the performance of the proposed OGMs compared with the ones by PCA and LDA. As the best performance is achieved with 95% variance of learning data kept both for PCA and LDA, we carried out PCA and LDA on OGMs only using this configuration, thus setting up the kept variance to 95% as well. As we can see from the table, all the performances when fusing the scores from the 8 orientations are improved by 4 to 5 points in the three experimental setups as compared to the figures displayed by PCA and LDA when they were directly applied to the raw hand vein images. These performances highlight that OGMs improve indeed the distinctiveness of hand vein images. The experiments with the verification scenario further demonstrate the benefit of OGMs instead of the raw original hand vein images.

5 Conclusion

In this paper, we introduce Oriented Gradient Maps as effective representations of NIR hand vein images in order to increase their distinctiveness. Using a holistic approach through both popular PCA and LDA, we carried out extensive experiments on the NCUT dataset and demonstrated the effectiveness of the proposed approach for the increase of discrimination power of vein patterns under the OGMs. In our future work, we are improving the matching scheme, for instance making use of both global and local features of hand vein patterns, to further bolster the recognition performance.

Acknowledgement

This work has been supported in part by the French National Research Agency (ANR) through the FAR 3D project under grant ANR-07-SESU-003.

References

[KuHG09] A. Kumar, M. Hanmandlu, and H. M. Gupta, "Online biometric authentication using hand vein pattern", IEEE Symposium on Computational Intelligence in Security and Defense Applications, 2009.

[MaWe91] P. MacGregor and R. Welford, "Veincheck: imaging for security and personal identification", Adv. Imaging, vol.6, no. 7, pp.52-56, 1991

[MaSp07] S. Malki and L. Spaanenburg, "Hand vein feature extracting using DT-CNNS", SPIE, vol.6590, 2007.

[LiFa04] C. Lin and K. Fan, "Biometric verification using thermal images of palm-dorsa vein patterns", IEEE Transaction on Circuits and Systems for Video Technology, vol.14, no.2, 2004.

[ZhWW08] S. Zhao, Y. Wang, and Y. Wang, "Biometric identification based on low quality hand vein pattern images", International Conference on Machine Learning and Cybernetics, vol.2, pp.1172-1177, 2008.

[KuVe09] A. Kumar, and K. V. Prathyusha, "Personal authentication using hand vein triangulation and knucle shape", IEEE Transactions on Image Processing, vol.18, no.9, pp. 2127-2136, 2009.

[MiNM04] N. Miura, A. Nagasaka, and T. Miyatake, "Feature extraction of finger-vein pattern based on repeated line tracking and its application to personal identification", Machine Vision and Applications, vol.15, pp.194-203, 2004.

[CrSm95] J. M. Cross and C. L. Smith, "Thermographic imaging of the subcutaneous vascular network of the back of the hand for biometric identification", 29th Annual International Carnahan Conference on Security Technology, Sanderstead, UK, 1995.

[WZYZ06] K. Wang, Y. Yuan, Z. Zhang, and D. Zhuang, "Hand vein recognition based on multisupplemental features of multi-classifier fusion decision", IEEE International Conference on Mechatronics and Automation, 2006

[WaLe06] L. Wang and G. Leedham, "Near- and far-infrared imaging for vein pattern biometrics", IEEE International Conference on Video Signal Based Surveillance, 2006.

[ZhWW07] S. Zhao, Y. Wang, and Y. Wang, "Extracting hand vein patterns from low-quality images: a new biometric technique using low-cost devices", 4th International Conference on Image and Graphics, pp.667-671, 2007.

[WLCS10] Y. Wang, K. Li, J. Cui, L. Shark, and M. Varley, "Study of hand-dorsa vein recognition", International Conference on Intelligent Computing, 2010.

[HWAW11] D. Huang, W. Ben Soltana, M. Ardabilian, Y. Wang, and L.Chen, "Textured 3D face recognition using biological vision-based facial representation and optimized weighted sum fusion," CVPR Workshop on Biometrics, 2011.

[EdIP97] S. Edelman, N. Intrator, and T. Poggio, T, "Complex cells and object recognition," Unpublished manuscript: http://kybele.psych.cornell.edu/~edelman/archive.html, 1997.

[Bada06] A. M. Badawi, "Hand vein biometric verification prototype: a testing performance and patterns similarity, International Conference on Image Processing, Computer Vision, and Pattern Recognition, 2006.

[DuHS01] R. O. Duda, P. E. Hart, and D. G. Stork, "Pattern classification", Wiley-Interscience, 2nd edition, 2001.